

Test of s-channel Helicity Conservation in Inelastic ρ^0
Diffraction in 20 GeV Photoproduction*

The SLAC Hybrid Facility Photon Collaboration

K. Abe^m, T.C. Bacone, J. Ballam^k, A.V. Bevane, H.H. Bingham^o, J.E. Brau^q,
K. Braune^k, D. Brick^b, W.M. Bugg^q, J.M. Butler^k, W. Camerone, H.O. Cohnⁱ,
G. Condo^q, D.C. Colley^a, S. Dadol, R. Diamond^d, P. Dingus^o, R. Erickson^k,
R.C. Field^k, B. Franek^j, N. Fujiwarah^h, R. Gearhart^k, T. Glanzmank,
I.M. Godfrey^e, J.J. Goldberg^l, A.T. Goshaw^c, G. Halle, E.R. Hancock^j,
T. Handler^q, H.J. Hargis^q, E.L. Hart^q, M.J. Harwine, K. Hasegawa^m,
R.I. Hulsizer^g, M. Jobes^a, G.E. Kalmus^j, D.P. Kelsey^j, T. Kitagaki^m, A. Levy^p,
P.W. Lucas^c, W.A. Mannⁿ, E. McCrory^c, R. Merenyiⁿ, R. Milburnⁿ, C. Milstene^p,
K.C. Moffeit^k, A. Napiernⁿ, S. Noguchi^h, F. Ochiai^f, S. O'Neale^a,
A.P.T. Palounek^c, I.A. Pless^g, P. Rankink, H. Sagawa^m, T. Satof, J. Schnepsⁿ,
S.J. Sewell^j, J. Shank^o, A.M. Shapiro^b, J. Shimony^q, R. Sugahara^f, A. Suzuki^f,
K. Takahashi^f, K. Tamai^m, S. Tanaka^m, S. Tether^g, D.A. Waide^a, W.D. Walker^c,
M. Widgoff^b, C.G. Wilkins^a, S. Wolbers^o, C.A. Woods^j, A. Yamaguchi^m,
R.K. Yamamoto^g, S. Yamashita^h, Y. Yoshimura^f, G.P. Yost^o, H. Yuta^m.

Submitted to
Physical Review D

* Work supported in part by the Department of Energy, contract DE-AC03-76SF00515, by the Japan-US Cooperative Research Project on High Energy Physics under the Japanese Ministry of Education, Science, and Culture, by the Science and Engineering Research Council (United Kingdom), by the US National Science Foundation, and by the US-Israel Academy of Sciences Commission for Basic Research.

- a. Birmingham University, Birmingham, B15 2TT, England
- b. Brown University, Providence, Rhode Island, 02912
- c. Duke University, Durham, North Carolina, 27706
- d. Florida State University, Tallahassee, Florida, 32306
- e. Imperial College, London, SW7 2BZ, England
- f. National Laboratory for High Energy Physics (KEK), Oho-machi, Tsukuba-gun, Ibaraki 305, Japan
- g. Massachusetts Institute of Technology, Cambridge, Massachusetts, 02139
- h. Nara Womens University, Kita-uoya, Nishi-Machi
Nara 630, Japan
- i. Oak Ridge National Laboratory, Oak Ridge, Tennessee, 37830
- j. Rutherford Appleton Laboratory, Didcot,
Oxon OX11 0OX, England
- k. Stanford Linear Accelerator Center, Stanford University,
Stanford, California, 94305
- l. Technion-Israel Institute of Technology, Haifa 32000, Israel
- m. Tohoku University, Sendai 980, Japan
- n. Tufts University, Medford, Massachusetts, 02155
- o. University of California, Berkeley, California, 94720
- p. University of Tel Aviv, Tel Aviv, Israel
- q. University of Tennessee, Knoxville, Tennessee, 37996

Test of s-channel Helicity Conservation in Inelastic ρ^0 Diffraction
in 20 GeV Photoproduction

The SLAC Hybrid Facility Photon Collaboration

Abstract

The reaction $\gamma p \rightarrow \rho^0_{\text{fast}} p \pi^+ \pi^-$ has been studied with the linearly polarized 20 GeV monochromatic photon beam at the SLAC Hybrid Facility to test the prediction of s-channel helicity conservation in inelastic diffraction for $t' < 0.4(\text{Gev}/c)^2$. In a sample of 1934 events from this reaction, the ρ^0 decay angular distributions and spin density matrix elements are consistent with s-channel helicity conservation, the $\pi^+ \pi^-$ mass shape displays the same skewing seen in the reaction $\gamma p \rightarrow p \pi^+ \pi^-$, and the $p \pi^+ \pi^-$ mass distribution compares well and scales according to the vector dominance model with that produced in $\pi^\pm p \rightarrow \pi^\pm_{\text{fast}} p \pi^+ \pi^-$.

INTRODUCTION

Conservation of s-channel helicity (SCHC) in hadronic diffraction has been of experimental¹⁻⁸ and theoretical⁹⁻¹¹ interest for over a decade. SCHC follows naturally from QCD-based models of the Pomeron such as two gluon exchange.¹² Evidence for SCHC has been reported in the elastic diffraction processes $\gamma p \rightarrow pp^1$ and $\pi N \rightarrow \pi N^2$. It has been speculated that it might also be valid in inelastic diffraction,⁹ but this is not found to be true in πp ,³ $K p$,⁴ and pp ,^{5,10} experiments. Thus, SCHC is no longer viewed as a general rule for inelastic diffraction, although evidence suggests that in some cases the inelastic diffraction which displays nonconservation of s-channel helicity may result from two production mechanisms, one of which exhibits SCHC^{6,7}. Furthermore, analysis based on the Deck model has explained the patterns of s- and t-channel helicity conservation in meson diffraction dissociation.¹¹

Polarized p-mesons produced by linearly polarized photons on hydrogen provide a good test of SCHC. Previous work has shown evidence for SCHC in inclusive inelastic ρ^0 photoproduction^{8,13}. If SCHC holds in the inelastic diffractive reaction $\gamma p \rightarrow \rho N^*$, the polar and azimuthal angular distributions of the ρ^0 decay in the helicity system will follow the well-known prediction¹⁴ $W(\cos \theta, \psi) = (3\sin^2\theta/8\pi)(1 + P_\gamma \cos 2\psi)$ independent of t . In what follows we report evidence of SCHC in $\gamma p \rightarrow \rho N^*$ from an analysis of a clean sample of 1934 such events produced in the SLAC Hybrid Facility exposed to a linearly polarized 20 GeV photon beam.

EXPERIMENTAL DETAILS

The experiment has been described in previous publications¹⁵⁻¹⁸. The linearly polarized monochromatic photon beam is formed by backscattering an ultraviolet laser beam from the SLAC 30 GeV primary electron beam. The backscattered photons have a 52 percent linear polarization. The SLAC Hybrid Facility consists of a 40-inch hydrogen bubble chamber, with its flashlamps triggered by signals from downstream detectors: proportional wire chambers,¹⁶ Cherenkov counters,¹⁷ and a lead glass wall¹⁸. The trigger accepts 88 ± 3 percent of the total cross section. The data presented here has been corrected on an event by event basis for the relatively small losses in the trigger efficiency. The average weight is 1.11 for the inelastic ρ^0 production events and the acceptance varies less than 20 percent over the t' , mass, and angle ranges of the events used in the reaction $\gamma p \rightarrow \rho^0_{\text{fast}} p \pi^+ \pi^-$.

EVIDENCE FOR DIFFRACTIVE INELASTIC ρ^0 PHOTOPRODUCTION

A sample of 6468 events having a 3-constraint fit to the reaction $\gamma p \rightarrow p \pi^+ \pi^+ \pi^- \pi^-$ with total energy between 15 and 20 GeV has been selected from the 300,000 hadronic events measured in this experiment. Figure 1a shows the two-pion effective masses for this final state; histogram A is the spectrum for all $\pi^+ \pi^-$ combinations (4 per event) while curve B is the sum of spectra for the two same-sign combinations. The 4-pion effective mass distribution, shown in figure 1b, is dominated by $\rho'(1600)$ production. Figure 2 gives the two pion momentum spectra for selections described below. From Figures 1 and 2 the following qualitative conclusions can be drawn:

- a: The $\pi^+ \pi^-$ mass-spectrum (histogram A figure 1a) shows a prominent ρ^0 signal which rises above the combinatorial background represented by histogram B.

b: The $\rho'(1600)$ signal is enhanced if only those $\pi^+\pi^-$ masses in the ρ^0 region ($M_{\pi^+\pi^-} < 1000$ MeV/c 2) are selected from histogram A in figure 1a; this effect is demonstrated by histogram B in figure 1b and indicates that there is a substantial ρ^0 signal coming from the decay of $\rho'(1600)$.

c: If the $\pi^+\pi^-$ system is further restricted to have momentum > 16 GeV/c and $|t'| = |t-t_{\min}| < 0.5$ (GeV/c) 2 the histogram C of figure 1b is obtained; the $\rho'(1600)$ signal is completely suppressed. This indicates that the ρ^0 's coming from $\rho'(1600)$ decay have a much softer momentum spectrum than those produced diffractively.

d: Curve A in figure 2 shows the momentum spectrum for $\pi^+\pi^-$ combinations having masses in the ρ^0 region ($M_{\pi^+\pi^-} < 1000$ MeV/c 2) with $|t'| < 1.0$ GeV/c 2 . Only the largest momentum $\pi^+\pi^-$ pair in each event is included. There is a broad contribution centered at 10 GeV/c with a hard component beyond 16 GeV/c; this supports the conclusion, in c above, that the ρ^0 are produced both diffractively and in $\rho'(1600)$ decay. Those arising from $\rho'(1600)$ decay are shown by curve B where the mass of the four pions is less than 2400 MeV/c. An estimate from this distribution of the non-diffractive background above 16 GeV/c yields 20 ± 5 percent.

e: The momentum spectrum shape for ρ^0 's produced elastically at the same incident gamma energy in the reaction $\gamma p \rightarrow p \pi^+\pi^-$ is shown in histogram C of figure 2 where there is a striking similarity with the hard component of histogram A, although histogram A is shifted to lower momenta by the more restrictive phase space resulting from the massive recoiling baryon system.

f: Finally, selecting only those events containing $\pi^+\pi^-$ pairs having momentum greater than 16 GeV/c² gives the mass spectrum shown in figure 3a which is clearly dominated by ρ^0 production and displays the mass-skewing exhibited in the quasi-elastic reaction $\gamma p \rightarrow \rho^0 p$ shown in figure 3b.

Using the selections described above, a sample of diffractively produced ρ^0 's has been isolated in the reaction $\gamma p \rightarrow p \pi^+\pi^-\pi^+\pi^-$, which is free from $\rho'(1600)$ feedthrough. The $\pi^+\pi^-$ mass distribution has been fitted by a curve representing the Söding model¹⁹ of the form:

$$\frac{d\sigma}{dm} = (f_{\rho D} + f_{\rho ND}) \sigma_{\rho}(m) + f_I I(m) + f_D D(m) + f_B B(m)$$

The four terms which contribute to this expression have the following origin:

a: The Breit-Wigner term representing ρ production, both diffractive and non-diffractive.

$$\sigma_{\rho}(m) = \frac{m}{q} \cdot \frac{\Gamma_{\rho}(m)}{(m_{\rho}^2 - m^2)^2 + m_{\rho}^2 \Gamma_{\rho}^2(m)} .$$

b: The Drell amplitude which represents the non-resonant $\pi^+\pi^-$ production from the photon.

$$D(m) = \frac{(m^2 - m_{\rho}^2)^2}{(m_{\rho}^2 - m^2)^2 + m_{\rho}^2 \Gamma_{\rho}^2(m)} .$$

c: A term representing the interference of the diffractive ρ amplitude with the Drell amplitude.

$$I(m) = \frac{m^2 - m_\rho^2}{(m_\rho^2 - m^2)^2 + m_\rho^2 \Gamma_\rho^2(m)}.$$

d: A polynomial non-resonant background.

$$B(m) = (m - 2m_\pi) + b(m - 2m_\pi)^2 + c(m - 2m_\pi)^3.$$

where b and c are parameters of the fit.

The parameters $f_{\rho D}$, $f_{\rho ND}$, f_I , f_D , and f_B represent the strengths of the following terms: the diffractive ρ^0 , the non-diffractive ρ^0 , the Drell mechanism, the Drell-rho interference, and the non-resonant background. A fit to the quasielastic distribution shown in Figure 3b was done with $f_{\rho ND}$ and f_B set to zero. The relative strengths of f_D , f_I , and $f_{\rho D}$ were then fixed in the inelastic fit. The integrated contribution from $f_{\rho ND}$ and f_B below 1000 MeV/c² was constrained to 20% as suggested earlier from Figure 2. In the above

$$\Gamma_\rho(m) = \Gamma_0 [q(m)/q(m_\rho)]^3 \frac{\rho(m)}{\rho(m_\rho)}$$

$$\rho(m) = [q^2(m) + q^2(m_\rho)]^{-1}$$

where q is the pion momentum in the center of mass of the dipion system and m_ρ and Γ_0 are the ρ^0 mass and width (769 ± 3 MeV/c² and 154 ± 5 MeV/c², respectively). The ρ^0 mass and width were allowed to vary in the final fit, the effects of which were included in the χ^2 with the above cited errors.

The Breit-Wigner term is symmetric around the position of the ρ mass; asymmetry about the ρ pole is produced by the interference term. Skewness in the

mass-spectrum is therefore evidence for a departure from pure ρ production.

Fractions of each process present have been fitted to the mass spectrum using a minimum χ^2 method; the full form shown above gives a χ^2 of 75 for 42 degrees of freedom compared to a value of 1088 if only the Breit-Wigner term is allowed to contribute.

In order to isolate the reaction $\gamma p \rightarrow \rho^0(p \pi^+\pi^-)$ we select only those events from Figure 3 with $M_{\pi\pi} < 1000$ MeV/c². Figure 4a shows the $p \pi^+\pi^-$ mass distribution for the pions opposite the selected $\pi\pi$ systems and compares this distribution with that of the diffractive reaction²⁰ $\pi^\pm p \rightarrow \pi^\pm(p \pi^+\pi^-)$ at 14 GeV/c. If we are indeed observing a diffractive reaction we would expect to be able to relate it to the pion-induced diffraction through the equation:

$$\sigma_{\gamma p \rightarrow \rho N^*} = \frac{\alpha}{2} \left(\frac{f_\rho^2}{4\pi} \right)^{-1} [\sigma_{\pi^+ p \rightarrow \pi^+ N^*} + \sigma_{\pi^- p \rightarrow \pi^- N^*}]$$

where $\frac{f_\rho^2}{4\pi} = 2.18$, determined by comparing quasi-elastic $\gamma p \rightarrow \rho^0 p$ to elastic $\pi^\pm p$ scattering²¹. Figure 4a shows a comparison of our data with such a renormalization of the π -induced diffraction. The agreement is very good in the relevant region ($M_{p\pi^+\pi^-} < 2000$ MeV/c²). Both distributions show similar features, with the photoproduction being about 10 percent less. The diffractive nature is further supported by observing the near equality of our measured cross section of $0.9 \pm 0.1 \mu\text{b}$ with the value reported²² for $\gamma p \rightarrow \rho^0 \Delta^{++} \pi^-$ at 9.3 GeV of $1.0 \pm 0.3 \mu\text{b}$. Figure 4b shows the $p \pi^+$ mass distribution from the $p \pi^+\pi^-$ system. The low mass $p \pi^+\pi^-$ system is clearly dominated by $\Delta^{++} \pi^-$. We have also observed a small component of $\Delta^0 \pi^+$, consistent with the expected 1/9 contribution for the decay of an N^* with isotopic spin 1/2. The t' distribution for the reaction has a slope which depends on the mass of the $p \pi^+\pi^-$ system as shown in Table I, with the largest slopes occurring for the smaller masses. This is the same dependence

To assess quantitatively the degree of s-channel helicity conservation for inelastic ρ^0 production, the density matrix elements of the ρ^0 decay in the helicity rest frame have been determined.

The decay angular distribution can be expressed in terms of nine independent measurable spin density matrix elements ρ_{ik}^a :

$$W(\cos\theta, \phi, \phi) = \frac{3}{4\pi} \left[\frac{1}{2}(1 - \rho_{00}^0) + \frac{1}{2}(3\rho_{00}^0 - 1)\cos^2\theta - \sqrt{2}\text{Re } \rho_{10}^0 \sin 2\theta \cos \phi - \rho_{1-1}^0 \sin^2\theta \cos 2\phi \right. \\ - P_Y \cos 2\phi (\rho_{11}^1 \sin^2\theta + \rho_{00}^1 \cos^2\theta - \sqrt{2}\text{Re } \rho_{10}^1 \sin 2\theta \cos \phi - \rho_{1-1}^1 \sin^2\theta \cos 2\phi) \\ \left. - P_Y \sin 2\phi (\sqrt{2}\text{Im } \rho_{10}^2 \sin 2\theta \sin \phi + \text{Im } \rho_{1-1}^2 \sin^2\theta \sin 2\phi) \right].$$

For transverse and linearly polarized photons, one expects, in the case of SCHC, that only two spin density matrix elements are non zero:

$$\rho_{1-1}^1 = \frac{1}{2} \quad \text{and } \text{Im } \rho_{1-1}^2 = -\frac{1}{2}.$$

The values for two t' bins are shown in Table II; these are from the angular distributions after removal of the 20 percent isotropic background. In general the helicity flip density matrices remain small as t' increases, e.g. $\rho_{00}^0 \sim 0$ for all t' , and the non-flip terms are consistent with their expected values.

CONCLUSION

In conclusion, we find that the features of ρ^0 decay in inelastic diffraction $\gamma p \rightarrow \rho N^*$ are consistent with s-channel helicity conservation as determined from the decay angular distributions and the spin density matrix elements. Furthermore, the inelastically produced ρ^0 displays the same mass skewing as the elastically produced ρ^0 . The nucleon dissociation mass spectrum is similar to that found in pion-induced nucleon diffraction dissociation and its cross section is similar to that calculated from the vector dominance model.

as in π -induced diffraction and similar to the variation observed with $\pi\pi$ mass in elastic $\pi\pi$ photoproduction.

To summarize, we have observed diffractive inelastic ρ^0 production as evidenced by the peripheral nature, the ρ -mass skewing, the similarity and scaling of the $p_{\pi^+\pi^-}$ mass distribution to π -induced diffraction, and the isotopic spin 1/2 behavior of the $\Delta\pi$ branching ratios.

THE TEST OF s-CHANNEL HELICITY CONSERVATION

To test SCHC of the ρ^0 we have examined the distributions of conventional helicity angles.²³ The polar angle of the π^+ in the ρ -rest frame relative to the ρ direction of flight is denoted by θ . The difference between the azimuthal angles (ϕ , the angle between the photon polarization vector and the production plane in the center of mass system, and ϕ , the azimuthal angle of the ρ decay in the ρ rest frame measured as the angle between the decay plane and the production plane) is denoted by Ψ ($\Psi = \phi - \phi$). If s-channel helicity is conserved the ρ will have helicity ± 1 and $W(\cos \theta, \Psi) = (\frac{3}{8\pi} \sin^2 \theta)(1 + P_\gamma \cos 2\Psi)$. $P_\gamma = 0.52$ is the calculated degree of photon polarization, verified by the elastic ρ measurements²⁴.

Figure 5 presents the distributions for $\cos \theta$ and Ψ for this reaction²⁵ with the further restriction, $720 \text{ MeV}/c^2 < M_{\pi\pi} < 820 \text{ MeV}/c^2$ (along with the previous cuts $P_{\pi^+\pi^-} > 16 \text{ GeV}/c$, $M_p_{\pi^+\pi^-} < 2200 \text{ MeV}/c^2$). The solid curves give the prediction of SCHC and include a contribution from 20 percent background which is assumed to be isotropic, $W(\cos \theta, \Psi) = \frac{1}{4\pi}$. This angular distribution for the background was found to be consistent with that of the $\pi^+\pi^-$ pairs in the region $P_{\pi^+\pi^-} \sim 10 \text{ GeV}/c$. There is good agreement with the expected SCHC behavior indicating that this reaction is dominated by SCHC.

ACKNOWLEDGEMENTS

We wish to thank the SLAC bubble chamber crew for their dedication to this experiment and the film scanners and measurers at the many institutions for their careful processing of the events. We especially thank Joe Murray for his work on the beam. We have benefitted from discussion of the theory of this reaction with F. J. Gilman. The work was supported by the Japan-US Cooperative Research Project on High Energy Physics under the Japanese Ministry of Education, Science, and Culture, the US Department of Energy, the Science and Engineering Research Council (United Kingdom), the US National Science Foundation, and the US-Israel Academy of Sciences Commission for Basic Research.

References

1. J. Ballam et al., Phys. Rev. Lett. 24, 960 (1970).
2. F. Halzen and C. Michael, Phys. Lett. 36B, 367 (1971); A. Delesquez et al., Phys. Lett. 40B, 77 (1972); G. Gozzika et al., Phys. Lett. 40B, 281 (1972); V. Barger and F. Halzen, Phys. Rev. Lett. 28, 194 (1972).
3. Yu. M. Antipov et al., Nucl. Phys. B63, 153 (1973).
4. F. Grard et al., Lett. Nuovo Cimento 2, 305 (1971); J. V. Beaupre et al., Phys. Lett. 34B, 160 (1971); B. Buschbeck et al., Nucl. Phys. B35, 511 (1971); J. V. Beaupre et al., Nucl. Phys. B47, 51 (1972); G.W. Brandenburg et al., Nucl. Phys. B45, 397 (1972); R. Barloutaud et al., Nucl. Phys. B59, 374 (1972).
5. N.G. Albrow et al., Nucl. Phys. B108, 1 (1976).
6. G. Berlad et al., Nucl. Phys. B78, 29 (1974).
7. P. Bosetti et al., Nucl. Phys. B101, 304 (1975).
8. E. Kogan et al., Nucl. Phys. B122, 383 (1977).
9. F. Gilman, J. Pumplin, A. Schwimmer and L. Stodolsky, Phys. Lett. 31B, 387 (1970).
10. J. Pumplin, Physica Scripta 25, 191 (1981).
11. E.L. Berger and J.T. Donohue, Phys. Rev. D15, 790 (1977).
12. J. Randa, XI International Winter Meeting on Fundamental Physics, 11-16 April, 1983, Toledo, Spain.
13. K. C. Moffeit et al., Phys. Rev. D5, 1603 (1972).
14. G. Wolf, Nucl. Phys. B26, 317 (1971).
15. K. Abe et al., Phys. Rev. D30, 1 (1984).
16. R.C. Field et al., Nucl. Instr. and Meth. 200, 237 (1982).
17. A. Bevan et al., Nucl. Instr. and Meth. 203, 159 (1982).
18. J.E. Brau et al., Nucl. Instr. and Meth. 196, 403 (1983).
19. D. Aston et al., Nucl. Phys. B209, 56 (1982); P. Söding, Phys. Lett. 19, 702 (1966).
20. G.B. Chadwick et al., Phys. Rev. D17, 1713 (1978).
21. for a review, see T.H. Bauer, R.D. Spital, D.R. Yennie, and F.M. Pipkin, Rev. Mod. Phys. 50, 261 (1978).

22. H.H. Bingham et al., Phys. Lett. 41B, 635 (1972).
23. K. Schilling, P. Seyboth, and G. Wolf, Nucl. Phys. B15, 397 (1970); B18, 332 (E)
24. K. Abe et al., Phys. Rev. Lett. 53, 751 (1984).
25. Twenty-two percent of the experiment was excluded from the angular distribution analysis (as in reference 24) since the ultra-violet laser photons had a deteriorated polarization.

Table Captions

Table I The slope b of the differential cross section ($\frac{dN}{dt} = Ae^{bt'}$) as a function of the ($p\pi^+\pi^-$) mass [for the four momentum transfer squared from the photon to the ρ^0 ($t' = t - t_{\min}$)] for $|t'| < 0.4$ (GeV/c) 2 .

Table II The spin density matrix elements for the diffractive ρ^0 meson in the helicity reference frame. These matrix elements have been corrected for the $20 \pm 5\%$ non-diffractive background in the final data sample. This background is assumed to have an isotropic angular distribution.

Table I

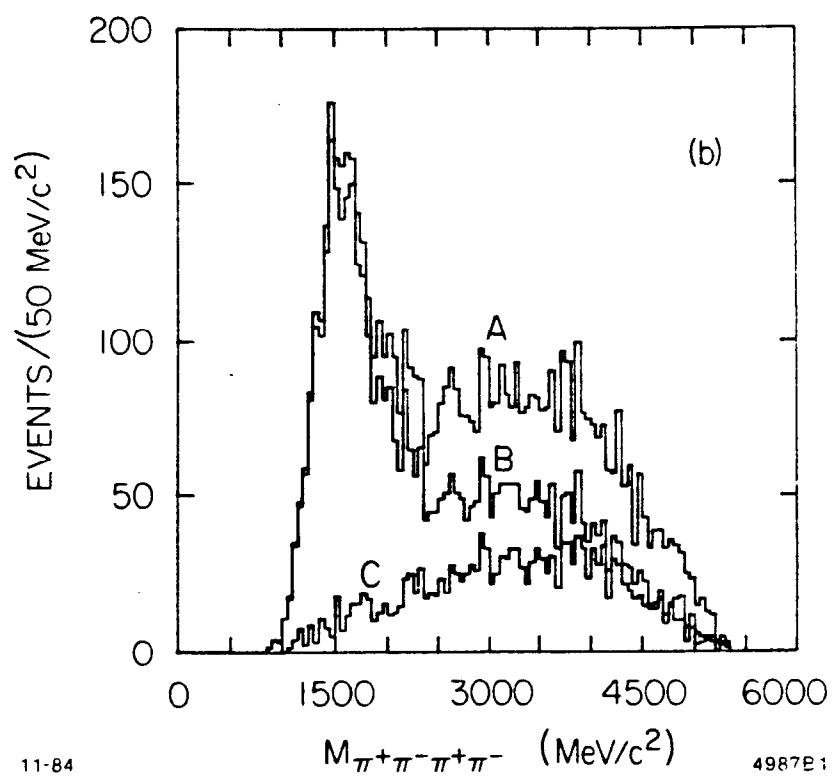
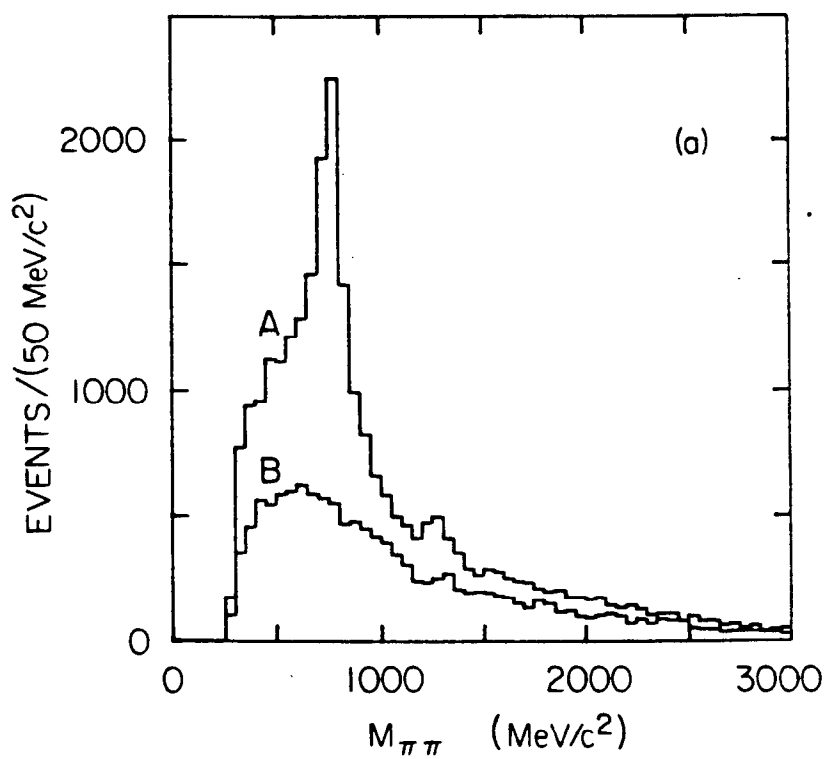
<u>M_p $\pi^+\pi^-$ (MeV/c²)</u>	<u>b(Gev/c)⁻²</u>
<1500	8.75 ± 0.49
1500 - 1600	10.66 ± 0.60
1600 - 1800	5.08 ± 0.30
1800 - 2100	5.53 ± 0.31
>2100	3.21 ± 0.23

Table II

	$0.0 < t' < 0.4$	$0.4 < t' < 1.0$
ρ_{00}^0	-0.01 ± 0.02	-0.01 ± 0.03
$\text{Re } \rho_{10}^0$	0.03 ± 0.02	-0.01 ± 0.05
ρ_{1-1}^0	-0.02 ± 0.03	-0.02 ± 0.06
ρ_{11}^1	0.05 ± 0.08	0.14 ± 0.19
ρ_{00}^1	0.04 ± 0.11	0.38 ± 0.18
$\text{Re } \rho_{10}^1$	0.10 ± 0.08	-0.10 ± 0.15
ρ_{1-1}^1	0.28 ± 0.11	0.61 ± 0.24
$\text{Im } \rho_{10}^2$	-0.05 ± 0.07	0.37 ± 0.17
$\text{Im } \rho_{1-1}^2$	-0.39 ± 0.12	-0.69 ± 0.24

Figure Captions

1. (a) The $\pi\pi$ mass distributions for 6468 events of the reaction $\gamma p \rightarrow p \pi^+\pi^+\pi^-\pi^-$. A is $\pi^+\pi^-$ and B is $\pi^\pm\pi^\pm$.
- (b) The 4 π mass distribution for the reaction. A is all 6468 events, B is the 4528 events with $M_{\pi^+\pi^-} < 1000 \text{ MeV}/c^2$ for at least one combination, and C is the 1614 events having one $\pi^+\pi^-$ combination with mass $< 1000 \text{ MeV}/c^2$, momentum $> 16 \text{ GeV}/c$, and $|t'_{\gamma+\pi^+\pi^-}| < 0.5 \text{ (GeV}/c)^2$.
2. The $\pi^+\pi^-$ momentum spectrum for $M_{\pi^+\pi^-} < 1000 \text{ MeV}/c^2$. A is for the largest momentum $\pi^+\pi^-$ with $|t'| < 1.0 \text{ GeV}/c^2$ (5102 events), B is for those which also have $M_{4\pi} < 2400 \text{ MeV}/c^2$ (2643 events), and C is the $\pi^+\pi^-$ momentum spectrum from the reaction $\gamma p \rightarrow p \rho^0 (\rho^0 \rightarrow \pi^+\pi^-)$ plotted to an arbitrary scale.
3. (a) The $\pi^+\pi^-$ mass distribution for the fast pairs selected as described in the text (2580 events, 2890 after weights). The fit is to the Söding model (see text).
- (b) Söding model fit to the $\pi^+\pi^-$ distribution for the reaction $\gamma p \rightarrow p p^0$ at 20 GeV/c .
4. (a) The $p \pi^+\pi^-$ mass distribution for the 1934 events (2144 after weights) with fast $\pi^+\pi^-$ pairs of mass $< 1000 \text{ MeV}/c^2$. The data points are from the reaction²⁰ $\pi^\pm p \rightarrow \pi^\pm_{\text{fast}} (p\pi^+\pi^-)$ where the total number of events with $M_{p\pi^+\pi^-} < 2200 \text{ MeV}/c^2$ has been renormalized by a VDM factor (see text).
- (b) The $p \pi^+$ mass distribution for the events in figure 4a.
5. The decay angular distributions of the $\pi^+\pi^-$ system in the helicity frame for the mass range $720 \text{ MeV}/c^2 < M_{\pi^+\pi^-} < 820 \text{ MeV}/c^2$. The data represent 532 events (588 after weights) and the superimposed curves are the expected distribution for SCHC including a 20 per cent background (with an isotropic angular distribution) and a photon polarization of 52 per cent.



11-84

4987E1

FIGURE 1

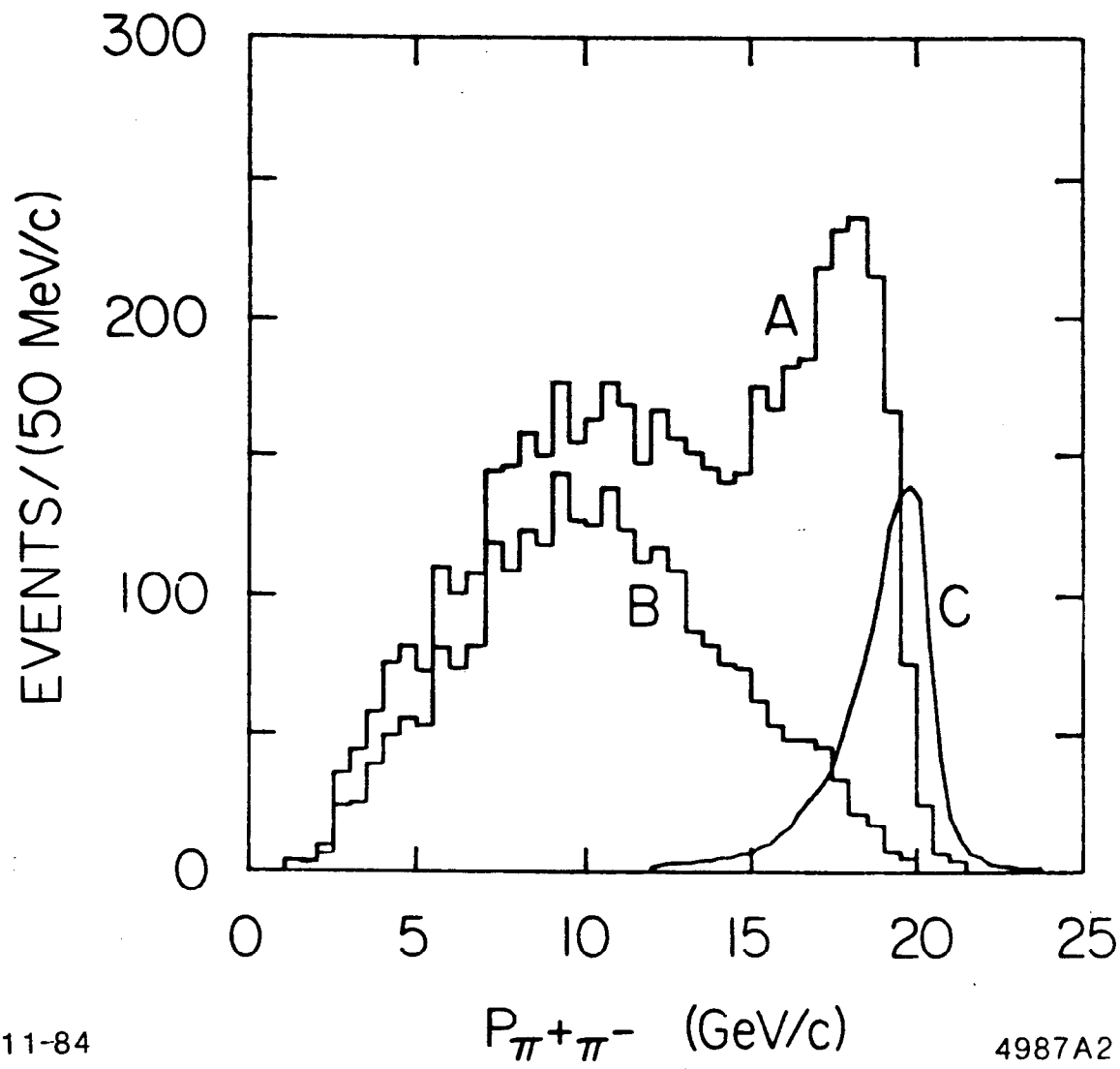


FIGURE 2

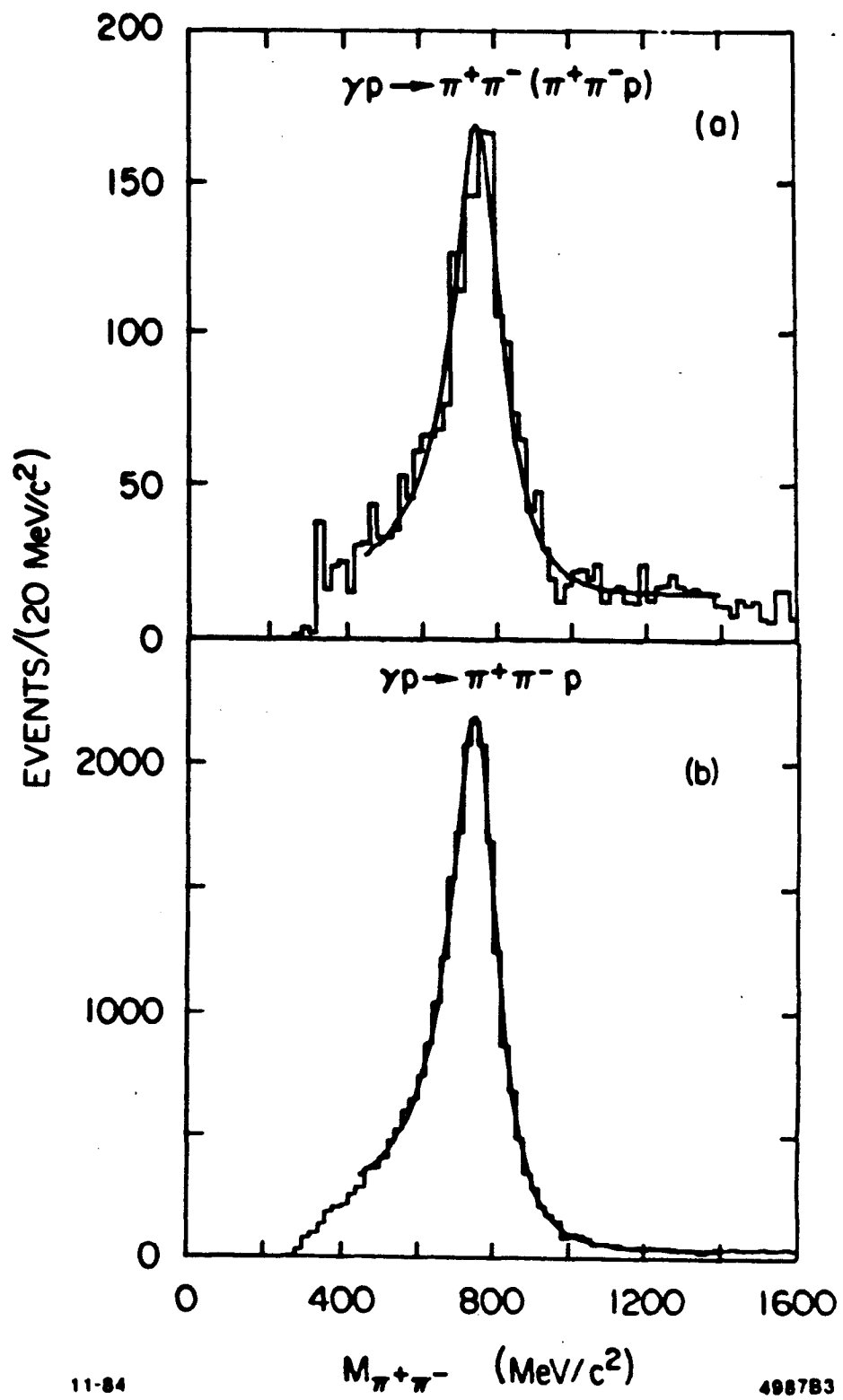


FIGURE 3

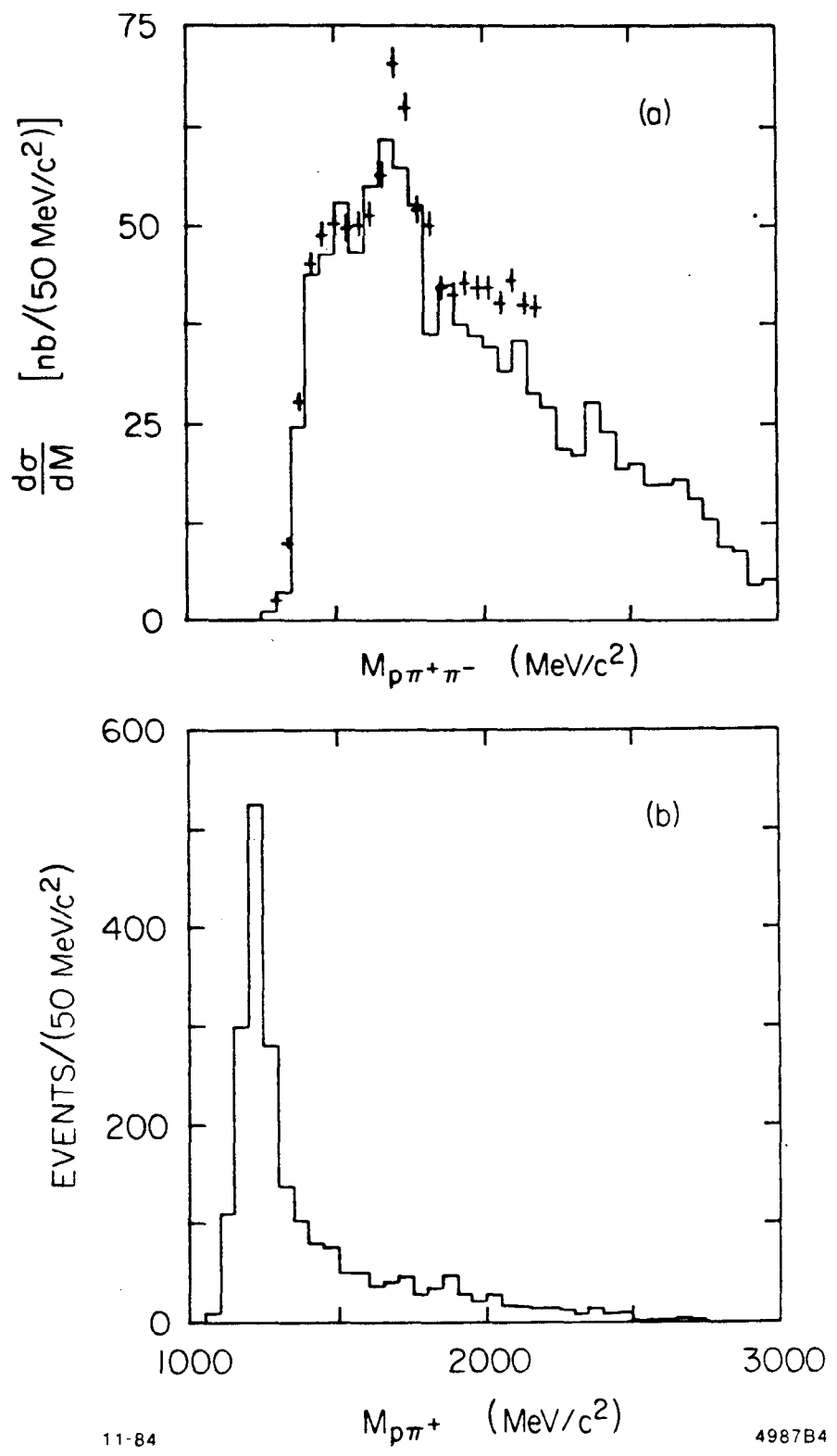


FIGURE 4

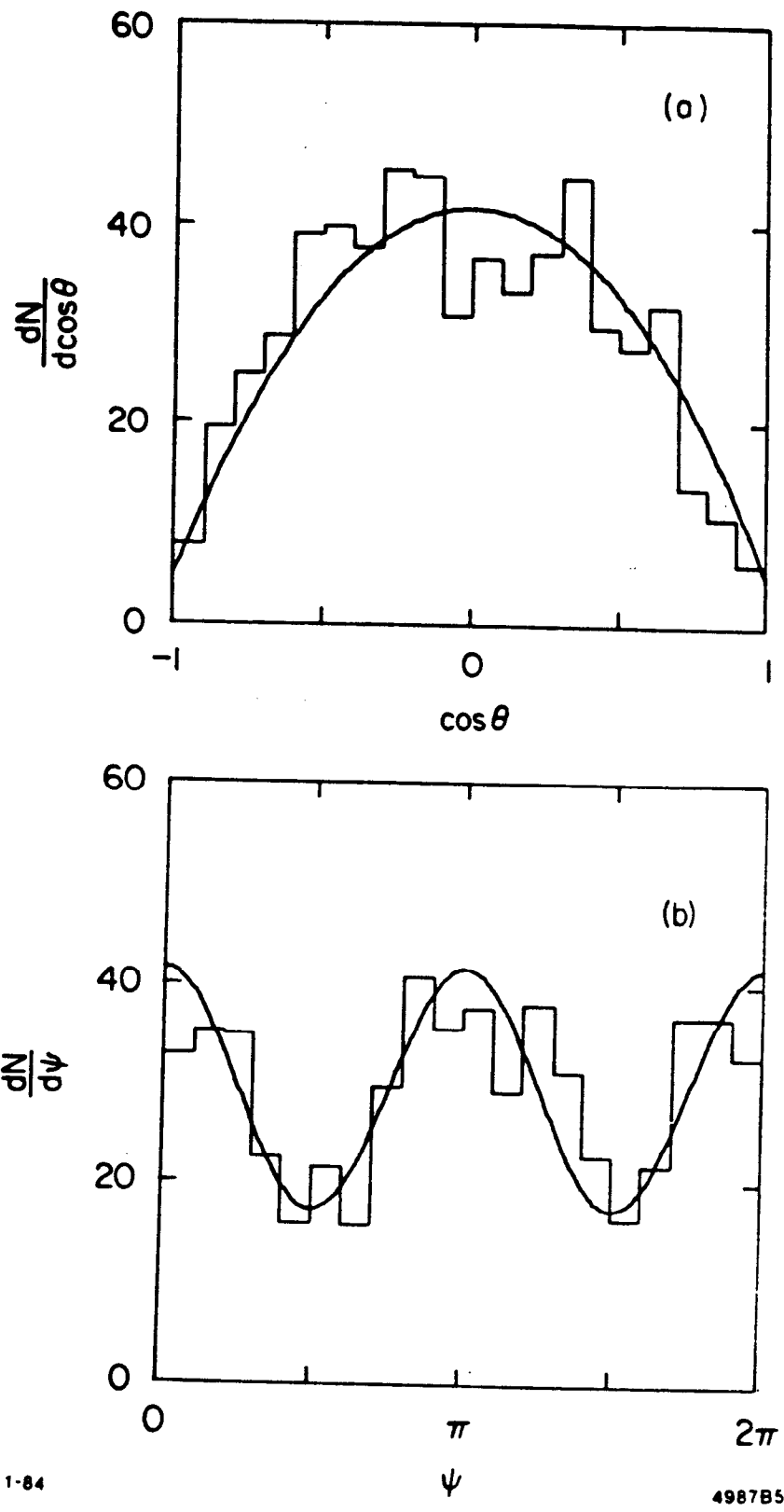


FIGURE 5

11-84

4987B5